YMTHE, Volume *29*

Supplemental Information

Circular RNA circPDE4D Protects against Osteoarthritis by Binding to miR-103a-3p and Regulating FGF18

Yizheng Wu, Zhenghua Hong, Wenbin Xu, Junxin Chen, Qingxin Wang, Jiaxin Chen, Weiyu Ni, Zixuan Mei, Ziang Xie, Yan Ma, Jiying Wang, Jianhong Lu, Chao Chen, Shunwu Fan, and Shuying Shen

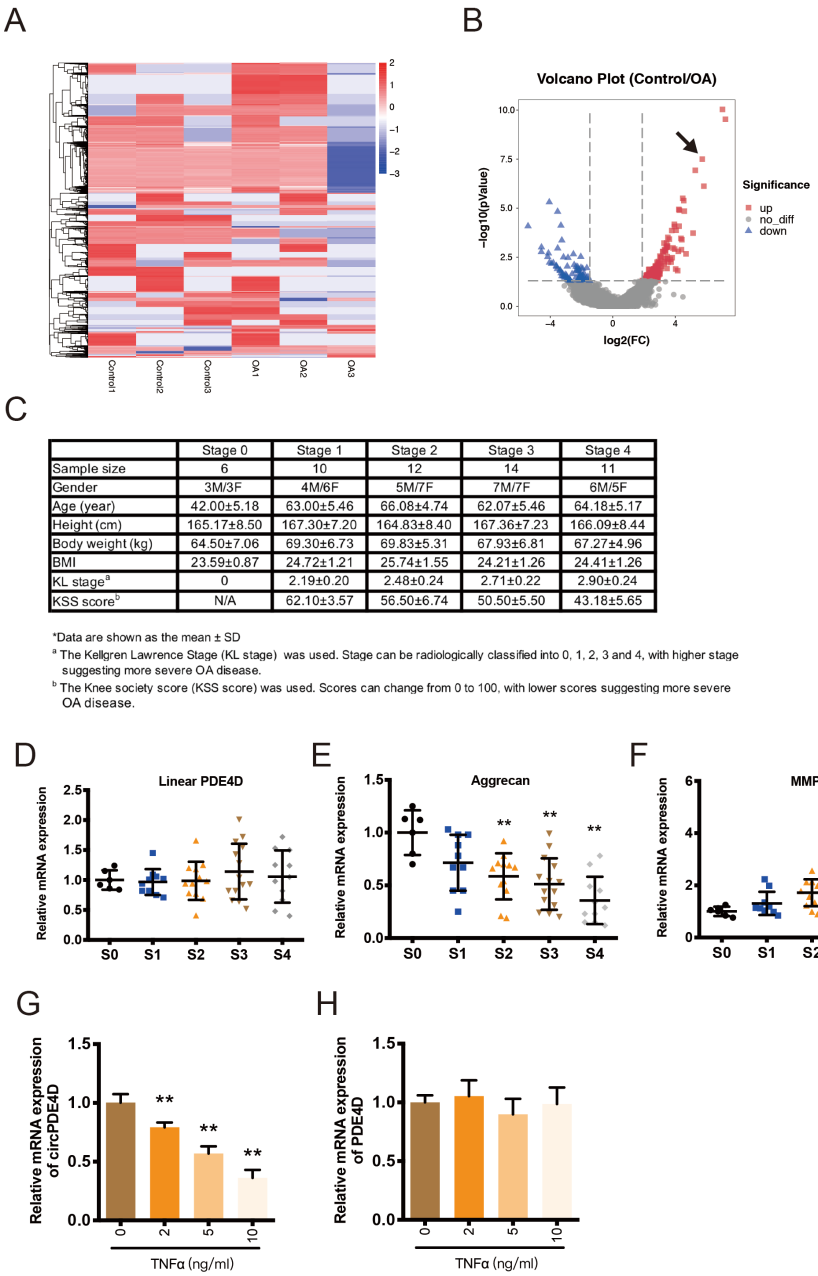

	Stage 0	Stage 1	Stage 2	Stage 3	Stage 4
Sample size	6	10	12	14	11
Gender	3M/3F	4M/6F	5M/7F	7M/7F	6M/5F
Age (year)	42.00±5.18	63.00±5.46	66.08±4.74	62.07±5.46	64.18±5.17
Height (cm)	165.17±8.50	167.30±7.20	164.83±8.40	167.36±7.23	166.09±8.44
Body weight (kg)	64.50±7.06	69.30±6.73	69.83±5.31	67.93±6.81	67.27±4.96
BMI	23.59±0.87	24.72±1.21	25.74±1.55	24.21±1.26	24.41±1.26
KL stage[a]	0	2.19±0.20	2.48±0.24	2.71±0.22	2.90±0.24
KSS score[b]	N/A	62.10±3.57	56.50±6.74	50.50±5.50	43.18±5.65

*Data are shown as the mean ± SD

[a] The Kellgren Lawrence Stage (KL stage) was used. Stage can be radiologically classified into 0, 1, 2, 3 and 4, with higher stage suggesting more severe OA disease.

[b] The Knee society score (KSS score) was used. Scores can change from 0 to 100, with lower scores suggesting more severe OA disease.

Supplementary Figure 1. Information on clinical cartilage specimens.

(A-B) Heatmap (A) and corresponding volcano plot (B) of differentially expressed circRNAs between control and OA cartilage specimens from our previous study. circPDE4D is indicated by a black arrow. The raw data are available on the NCBI SRA database (SRA accession number: PRJNA516555). (C) Information on the human specimens, including size, gender, age, height, body weight, BMI, KL stage and KSS score. (D-F) Expression of linear PDE4D, Aggrecan and MMP3 in 53 human cartilage specimens obtained by qRT-PCR analysis. (G-H) The expression of circPDE4D and linear PDE4D in human primary chondrocytes (HCs) stimulated with TNFα at concentrations of 0, 2, 5, or 10 ng/ml for 24 h was determined by qRT-PCR. The data were obtained from three independent donors (presented as the means ± SDs) (G-H) (*P<0.05 and **P<0.01 vs the control or indicated group). The data were analyzed by one-way ANOVA followed by the Bonferroni test (D-F) or two-tailed t-tests (G-H).

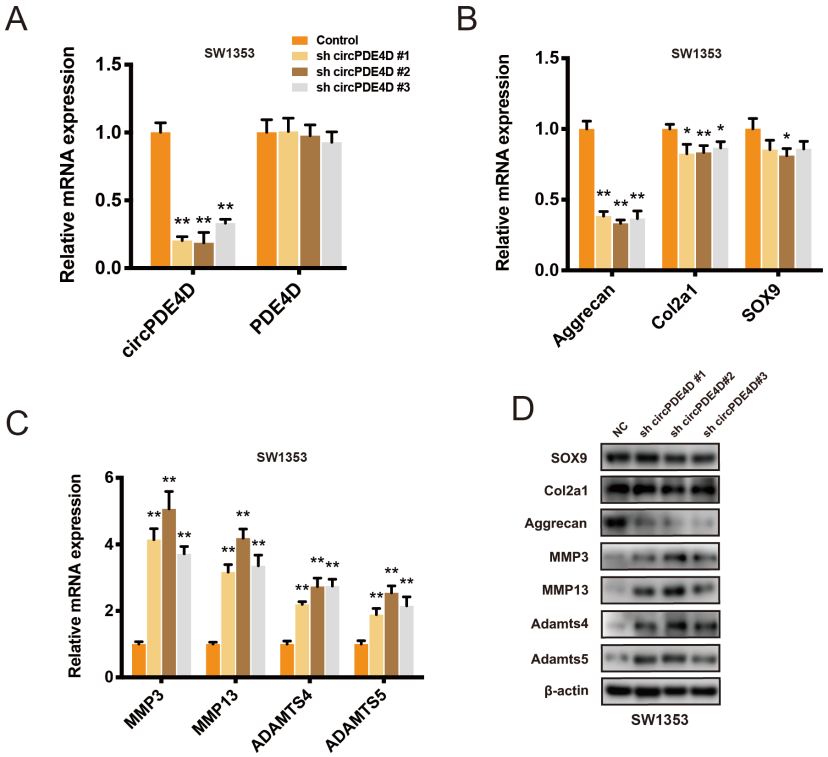

Supplementary Figure 2. The knockdown of circPDE4D induces matrix degradation in SW1353 cells.

(A) SW1353 cells were transfected with sh-circPDE4D #1, #2, #3 or NC and then used for qRT-PCR analysis. The histogram demonstrates the changes in the expression of circPDE4D and linear PDE4D. (B-C) SW1353 cells were stably transfected with sh-circPDE4D #1, #2, #3 or negative control, and the expression of Col2a1, Aggrecan, SOX9, MMP3, MMP13, ADAMTS4, and ADAMTS5 was evaluated by qRT-PCR. (D) The protein levels of SOX9, Col2a1, Aggrecan, MMP3, MMP13, ADAMTS4, and ADAMTS5 in stable SW1353 cells were evaluated by Western blotting. The data were obtained from three independent experiments (presented as the means ± SDs) (A-C) or were representative of three independent experiments with similar results (D). (*P<0.05 and **P<0.01 vs the control or indicated group) The data were analyzed by two-tailed t-tests (A-C).

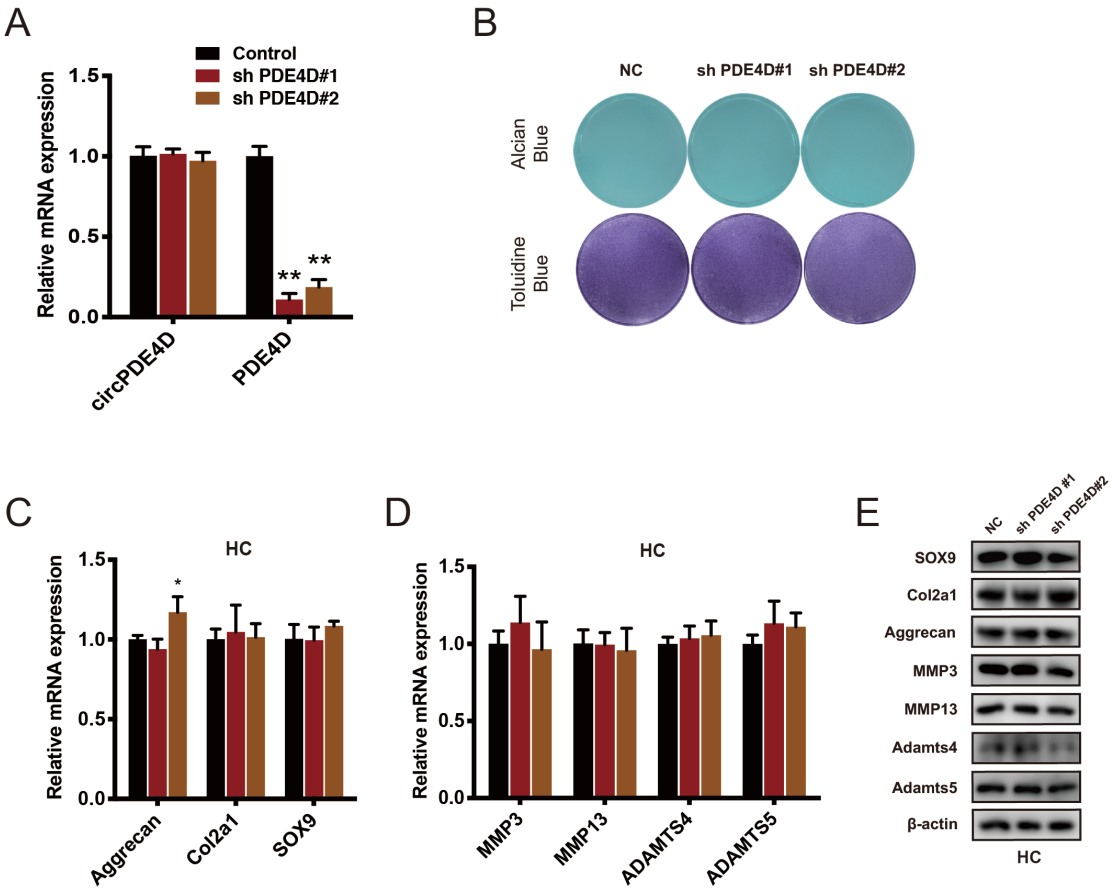

Supplementary Figure 3. Linear PDE4D is not related to matrix degradation. (A) HCs were stably transfected with sh-PDE4D #1, #2 or negative control. The histogram demonstrates the changes in the expression of circPDE4D and PDE4D. (B) The accumulation of proteoglycans was measured by Alcian blue and toluidine blue staining. (C-E) The expression of Col2a1, Aggrecan, SOX9, MMP3, MMP13, ADAMTS4, and ADAMTS5 at the mRNA and protein levels in HCs was evaluated by qRT-PCR and Western blotting. The data were obtained from three independent donors (presented as the means ± SDs) (A, C and D) or were representative of three independent experiments with similar results (B and E). (*P<0.05 and **P<0.01 vs the control or indicated group) The data were analyzed by two-tailed t-tests (A, C and D).

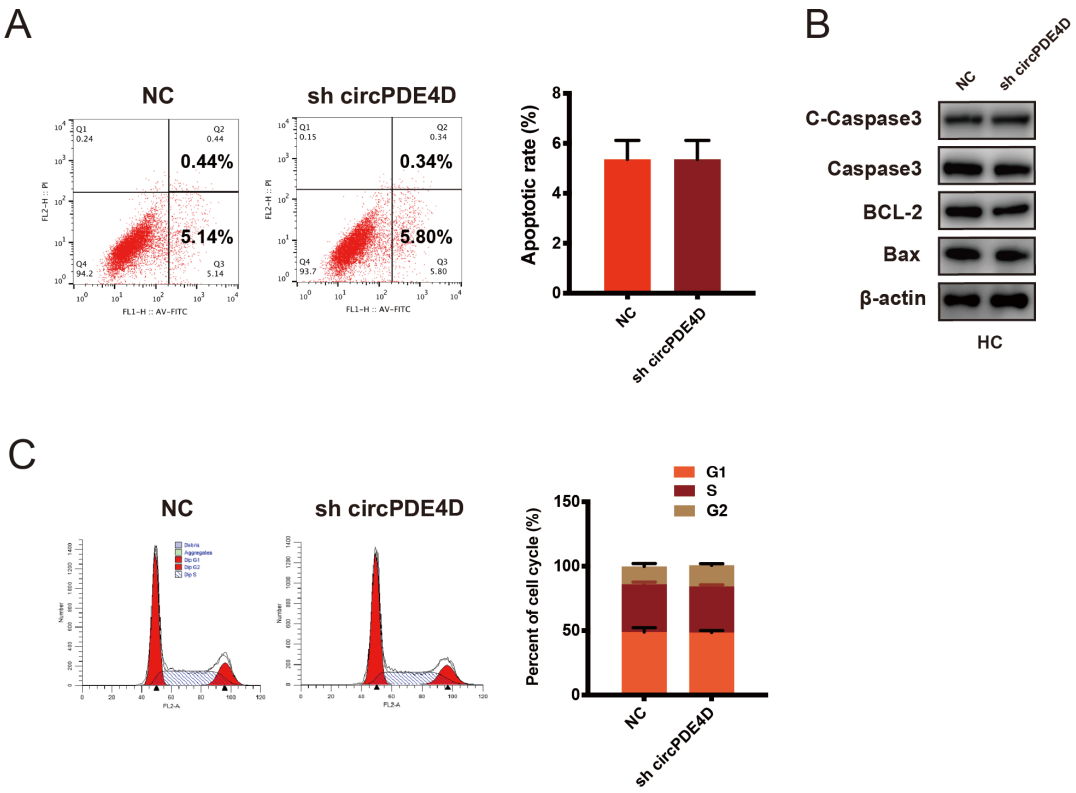

Supplementary Figure 4. circPDE4D is not related to apoptosis or the cell cycle. (A) Stable HCs were collected, stained with Annexin V-FITC and PI, and subjected to flow cytometry detection. Representative images and histograms are shown. (B) The expression of apoptosis-associated proteins (cleaved-Caspase 3, Caspase 3, BCL-2 and Bax) was evaluated by Western blotting. (C) The proportions of circPDE4D-knockdown HCs and their matched control cells at different phases of the cell cycle (G1, S and G2) were evaluated by flow cytometry. The data were obtained from three independent experiments with three independent donors (presented as the means ± SDs) (A and C) or were representative of three independent experiments with similar results (B). (*P<0.05 and **P<0.01 vs the control or indicated group). The data were analyzed by two-tailed t-tests (A and C).

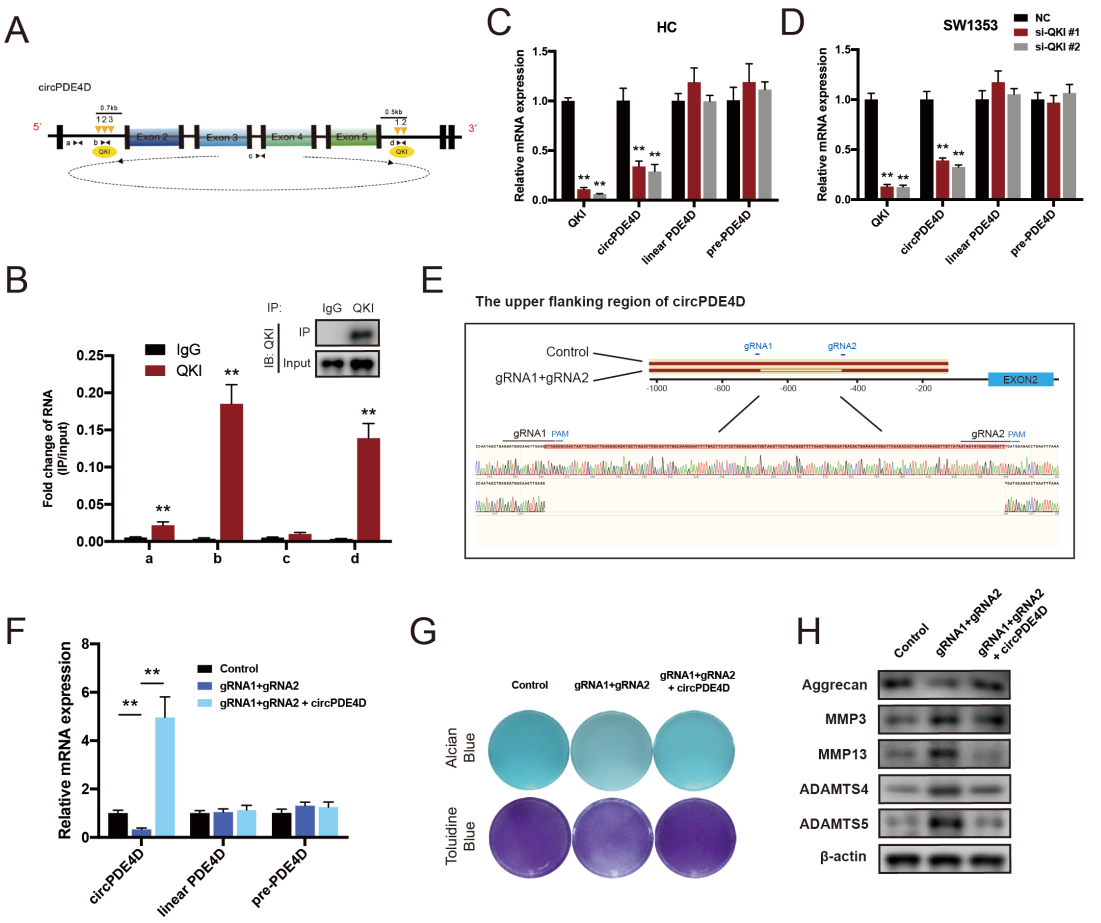

Supplementary Figure 5. Blocking the circPDE4D signal induces OA phenotypes in SW1353 cells.

(A) Schematic diagram of QKI response elements (QREs) in the flanking regions of circPDE4D. a, b, c and d respectively represent the primers in the remote region, upperstream flanking, splicing junction and downstream flanking region of circPDE4D. (B) The corresponding mRNAs in (A) were pulled by QKI and IgG and detected by RNA immunoprecipitation assay followed by qRT-PCR. (C-D) The relative mRNA levels of circPDE4D, linear PDE4D and pre-PDE4D after QKI knockdown were detected by qRT-PCR. (E) Sanger sequencing confirming the gene editing in the upper flanking region containing all the QREs by CRISPR/Cas9. (F) qRT-PCR indicated the expression of circPDE4D, linear PDE4D and pre-PDE4D after CRISPR/Cas9 or co-overexpression of circPDE4D. (G) Alcian blue and toluidine blue staining in the corresponding treatments were measured in SW1353. (H) The protein levels of Aggrecan, MMP3, MMP13, ADAMTS4 and ADAMTS5 were evaluated by Western blotting. The data were obtained from three independent experiments (presented as the means ± SDs) (B-D and F) or were representative of three independent experiments with similar results (G and H). (*P<0.05 and **P<0.01 vs the control or indicated group). The data were analyzed by two-tailed t-tests (B-D and F).

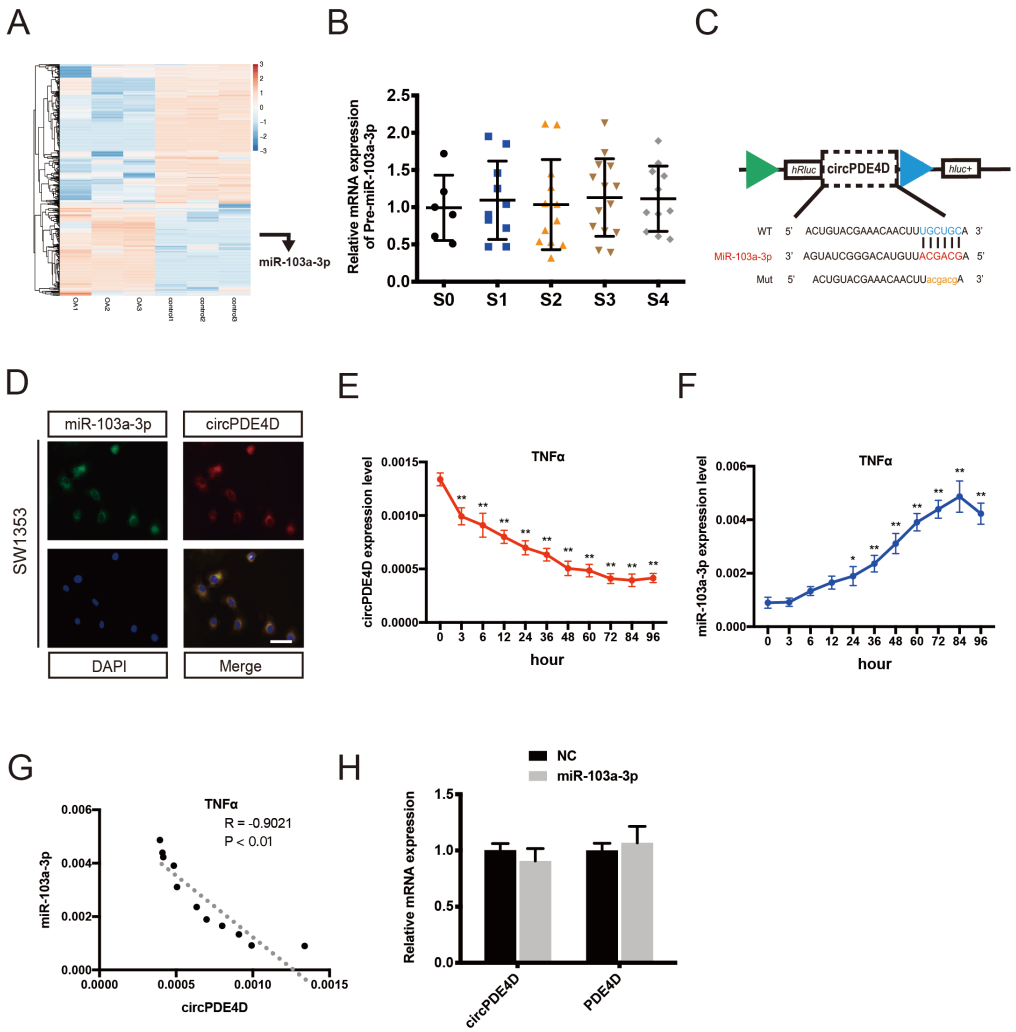

Supplementary Figure 6. miR-103a-3p expression and the correlation analysis. (A) miRNA sequencing of OA and normal cartilage specimens in our previously reported study. The raw data can be found at the NCBI SRA database (SRA accession number: PRJNA516556). (B) Abundances of pre-miR-103a-3p in clinical cartilage tissues. (C) Schematic illustration demonstrating the complementary miR-103a-3p seed sequence with circPDE4D. Lower letters indicate mutated nucleotides. (D) FISH images showing the colocalization of circPDE4D and miR-103a-3p in SW1353 cells. miR-103a-3p probes were labeled with Alexa Fluor 488. The circPDE4D probes were labeled with CY3. Nuclei were stained with DAPI. Scale bar: 20 μm. (E-F) Expression of circPDE4D (normalized to β-actin) and miR-103-3p (normalized to U6) after TNFα stimulation for different time points. (G) Pearson correlation analysis of circPDE4D and miR-103a-3p after TNFα stimulation for different time points (Pearson r=–0.9021; P<0.01). (H) The mRNA expression of circPDE4D and PDE4D after miR-103a-3p overexpression was detected by qRT-PCR. The data were obtained from three independent experiments with three independent donors (presented as the means ± SDs) (E, F and H) or were representative of three independent experiments with similar results (D). (*P<0.05 and **P<0.01 vs the control or indicated group). The data were analyzed by one-way ANOVA followed by the Bonferroni test (B, E and F) or two-tailed t-test (H).

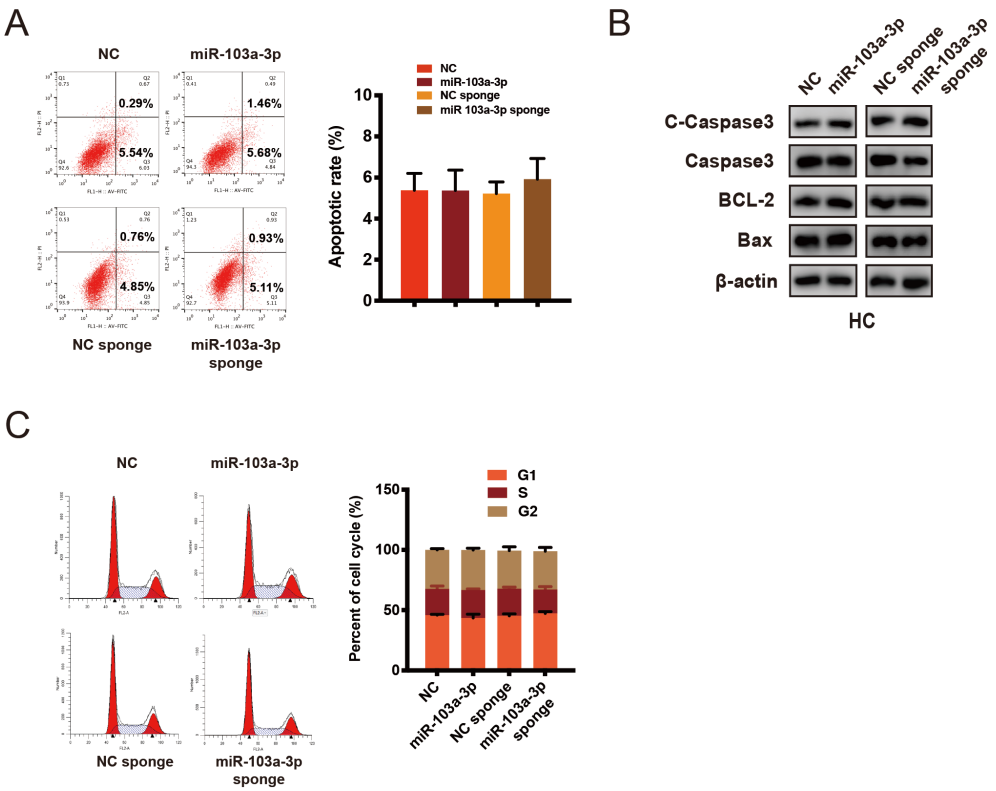

Supplementary Figure 7. miR-103a-3p is not related to apoptosis or the cell cycle. (A) HCs were transfected with miR-103a-3p, miR-103a-3p sponge or its negative control, stained with Annexin V-FITC and PI, and then subjected to flow cytometry detection. Representative images and histograms are shown. (B) The expression of apoptosis-associated proteins (cleaved-Caspase 3, Caspase 3, BCL-2 and Bax) was evaluated by Western blotting. (C) The proportions of cells at different cell cycle phases were evaluated by flow cytometry. The data were obtained from three independent experiments with three independent donors (presented as the means ± SDs) (A and C) or were representative of three independent experiments with similar results (B). (*P<0.05 and **P<0.01 vs the control or indicated group). The data were analyzed by two-tailed t-tests (A and C).

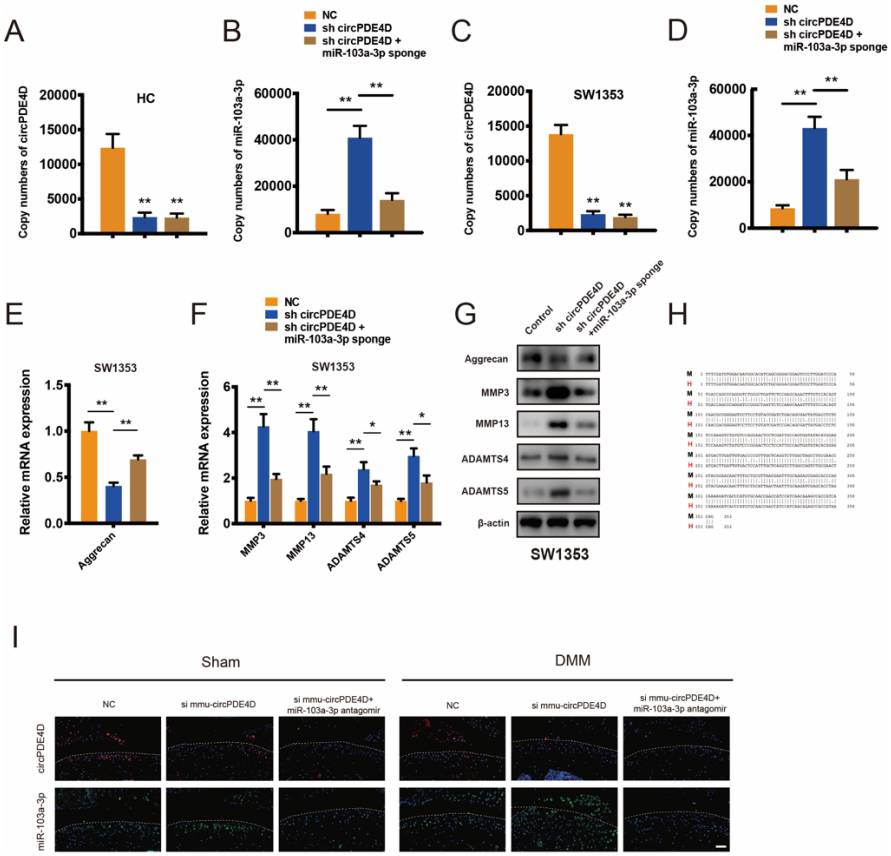

Supplementary Figure 8. miR-103a-3p reverses sh-circPDE4D-induced matrix degradation.

(A-B) HCs were stably transfected with empty vector (NC) or sh-circPDE4D or cotransfected with both sh-circPDE4D and miR-103a-3p sponge. The expression of circPDE4D and miR-103a-3p in HCs was evaluated by qRT-PCR. β-actin was used as an internal reference for mRNA, and U6 was used as an internal reference for miRNA. (C-D) SW1353 cells were stably transfected with empty vector (NC) or sh-circPDE4D or cotransfected with both sh-circPDE4D and miR-103a-3p sponge. The mRNA levels of circPDE4D and miR-103a-3p are shown in the histograms. (E-F) The mRNA expression of Aggrecan, MMP3, MMP13, ADAMTS4, and ADAMTS5 was evaluated by qRT-PCR. (G) The protein expression of Aggrecan and MMP3, MMP13, ADAMTS4, and ADAMTS5 was determined by Western blotting. (H) Sequence alignment of human circPDE4D (H) and the mouse circPDE4D homolog (M). (I) The expression of circPDE4D and miR-103a-3p in mouse cartilage was detected by FISH. miR-103a-3p probes were labeled with Alexa Fluor 488. Mmu-circPDE4D probes were labeled with CY3. Nuclei were stained with DAPI. Scale bar: 50 μm. The data were obtained from three independent experiments (presented as the means ± SDs) (A-F) or were representative of three independent experiments with similar results (G and I). (*P<0.05 and **P<0.01 vs the control or indicated group) The data were analyzed by two-tailed t-tests (A-F).

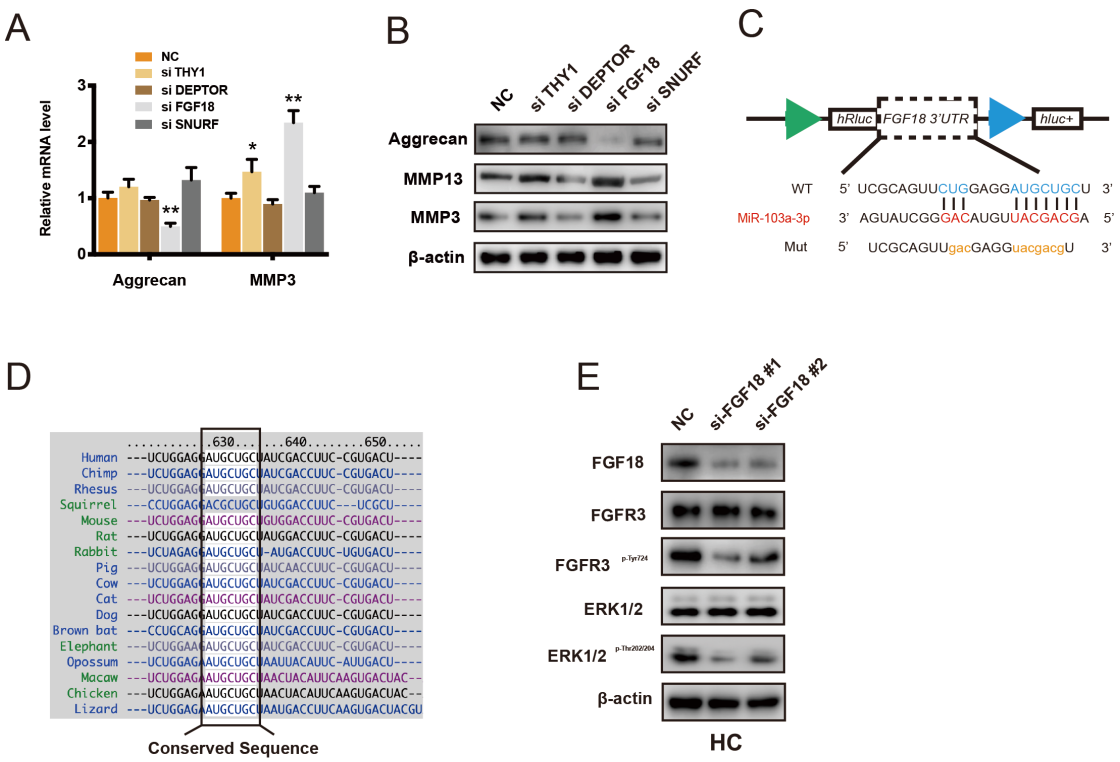

Supplementary Figure 9. FGF18 functions downstream of miR-103a-3p and plays a protective role in OA development.

(A) HCs were transfected with si-THY1, si-DEPTOR, si-FGF18, si-SNURF or negative control, and the changes in Aggrecan and MMP3 expression were evaluated by qRT-PCR. (B) Protein expression of Aggrecan, MMP3 and MMP13 after the knockdown of THY, DEPTOR, FGF18 or SNURF. (C) Schematic illustration demonstrating the complementary miR-103a-3p seed sequence with the FGF18 3'UTR. Lowercase letters indicate mutated nucleotides. (D) Sequence alignment of a putative miR-103a-3p-binding site within the 3'UTR of FGF18 mRNA revealed a high level of sequence conservation and complementarity with miR-103a-3p across vertebrates. (E) The protein expression of FGF18 and its downstream genes, including FGFR3, FGFR3$^{p\text{-}Tyr724}$, ERK1/2, and ERK1/2$^{p\text{-}Thr202/204}$, was determined by Western blotting. The data were obtained from three independent experiments with three independent donors (presented as the means ± SDs) (A) or were representative of three independent experiments with similar results (B and E). (*P<0.05 and **P<0.01 vs the control or indicated group) The data were analyzed by two-tailed t-tests (A).

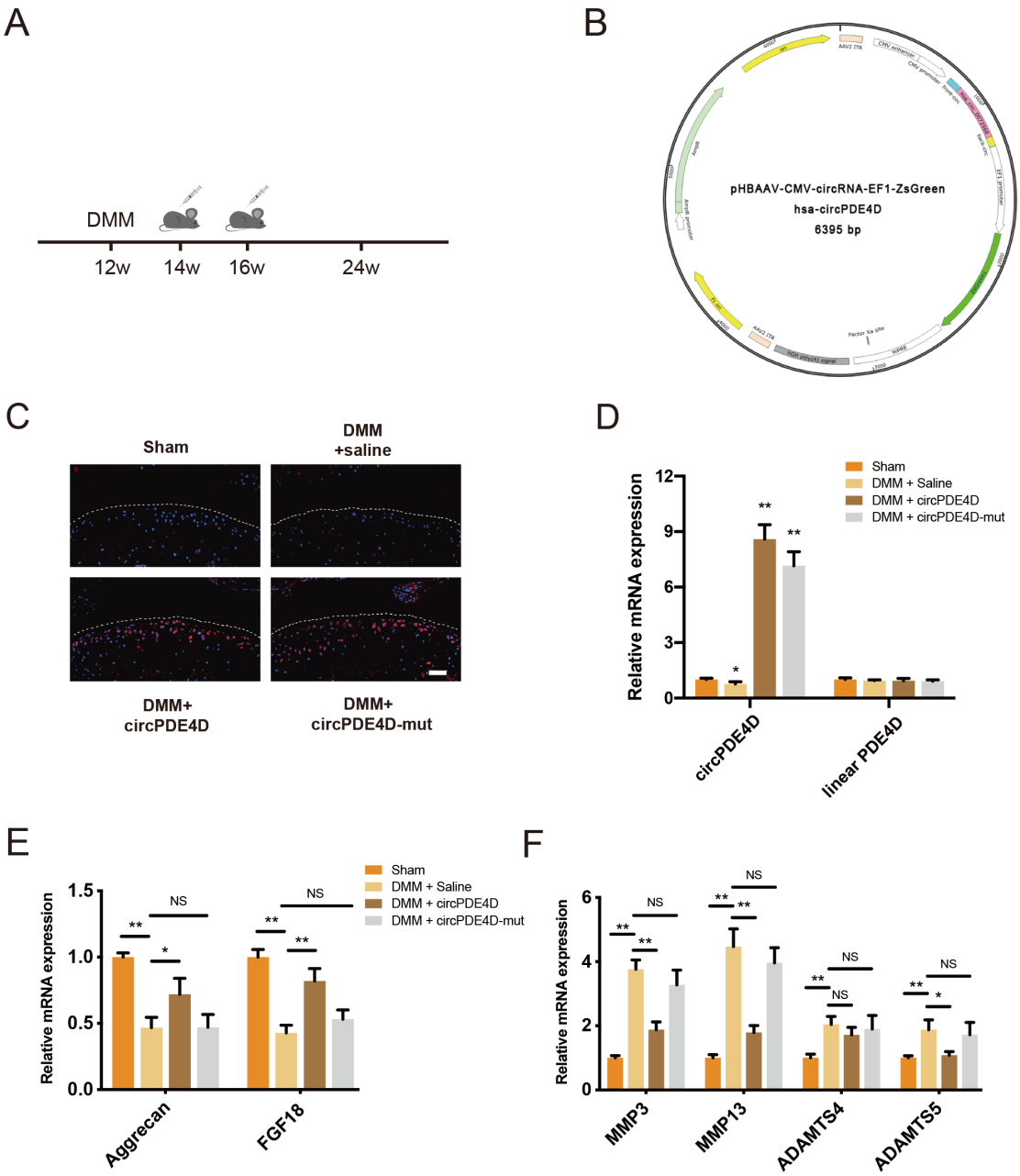

Supplementary Figure 10. Role of circPDE4D in the mouse DMM model.
(A) Schematic diagram demonstrating the timeline of the animal experiments. (B) Detailed information on the AAV. (C) The expression of circPDE4D (red) in mouse articular cartilage was detected. Representative images of FISH are shown. Scale bar: 50 μm. (D) The mRNA expression of circPDE4D and linear PDE4D in mouse cartilage was detected by qRT-PCR. (E-F) The expression of FGF18, catabolic enzymes (MMP3, MMP13, ADAMTS4 and ADAMTS5), and GAG composition (Aggrecan) in mouse cartilage tissues was determined by qRT-PCR. The data were presented as the means ± SDs (D-F) or were representative of three independent experiments with similar results (C). (*P<0.05 and **P<0.01 vs the control or indicated group) The data were obtained by two-tailed t-tests (D-F).

Supplemental Table 1 The information of patients

6 clinical cartilage tissues at stage 0						
Gender	Age (year)	Height (cm)	Weight (kg)	BMI	KL stage	KSS score
Female	40	155	54	22.48	0	N/A
Male	42	173	69	23.05	0	N/A
Female	48	157	58	23.53	0	N/A
Female	35	161	65	25.08	0	N/A
Male	39	171	69	23.60	0	N/A
Male	48	174	72	23.78	0	N/A
10 clinical cartilage tissues at stage 1						
Gender	Age (year)	Height (cm)	Weight (kg)	BMI	KL stage	KSS score
Male	63	176	76	24.54	2.3	66
Male	68	179	82	25.59	1.9	65
Male	70	170	68	23.53	2.5	67
Female	59	162	67	25.53	2.1	57
Female	59	162	69	26.29	2.2	65
Male	73	175	72	23.51	2.3	61
Female	59	158	59	23.63	2.2	62
Female	62	165	72	26.45	2.4	57
Female	57	162	61	23.24	1.9	61
Female	60	164	67	24.91	2.1	60
12 clinical cartilage tissues at stage 2						
Gender	Age (year)	Height (cm)	Weight (kg)	BMI	KL stage	KSS score
Male	69	167	71	25.46	2.5	56
Male	72	175	76	24.82	2.1	60
Female	73	165	68	24.98	2.5	43
Female	65	158	69	27.64	2.7	59
Female	63	157	62	25.15	2.1	68
Male	66	179	81	25.28	2.9	61
Female	71	155	66	27.47	2.3	63
Male	58	174	69	22.79	2.7	51
Female	59	161	73	28.16	2.6	53
Male	66	172	72	24.34	2.5	50
Female	64	156	63	25.89	2.3	54
Female	67	159	68	26.90	2.6	60
14 clinical cartilage tissues at stage 3						
Gender	Age (year)	Height (cm)	Weight (kg)	BMI	KL stage	KSS score
Male	59	176	70	22.60	2.7	48
Male	62	172	72	24.34	2.6	59
Male	69	181	80	24.42	2.7	59
Female	64	159	62	24.52	2.9	52
Female	70	166	67	24.31	2.9	44

Male	57	172	72	24.34	3.1	45
Female	54	162	71	27.05	3.1	49
Male	66	175	79	25.80	2.4	53
Female	55	164	62	23.05	2.7	45
Male	61	168	69	24.45	2.4	48
Female	67	164	59	21.94	2.5	49
Male	58	168	67	23.74	2.7	45
Female	69	161	64	24.69	2.6	60
Female	58	155	57	23.73	2.6	51
11 clinical cartilage tissues at stage 4						
Gender	Age (year)	Height (cm)	Weight (kg)	BMI	KL stage	KSS score
Female	66	155	59	24.56	3.2	41
Male	69	167	67	24.02	2.9	37
Male	71	169	66	23.11	3.1	45
Female	67	158	63	25.24	2.6	38
Male	69	176	69	22.28	2.8	37
Male	62	174	75	24.77	3.2	49
Female	61	160	65	25.39	2.9	49
Male	55	177	71	22.66	2.7	52
Female	67	154	62	26.14	2.9	37
Female	62	164	69	25.65	2.5	42
Male	57	173	74	24.73	3.1	48
Other cartilage tissues used for primary chondrocytes culture						
Gender	Age (year)	Height (cm)	Weight (kg)	BMI	KL stage	KSS score
Male	57	175	75	24.49	2.1	63
Male	62	174	73	24.11	2.4	58
Male	67	172	73	24.68	2.6	58
Female	64	162	62	23.62	2.7	54
Female	59	158	62	24.84	2.2	62
Male	62	174	69	22.79	2.8	49
Female	66	168	63	22.32	2.7	54
Male	65	165	60	22.04	2.5	55
Female	61	156	58	23.83	2.3	59